ISCI, Volume *19*

Supplemental Information

Safety of Whole-Body Abrogation of the TRF1 Shelterin Protein in Wild-Type and Cancer-Prone Mouse Models

Leire Bejarano, Jessica Louzame, Juán José Montero, Diego Megías, Juana M. Flores, and Maria A. Blasco

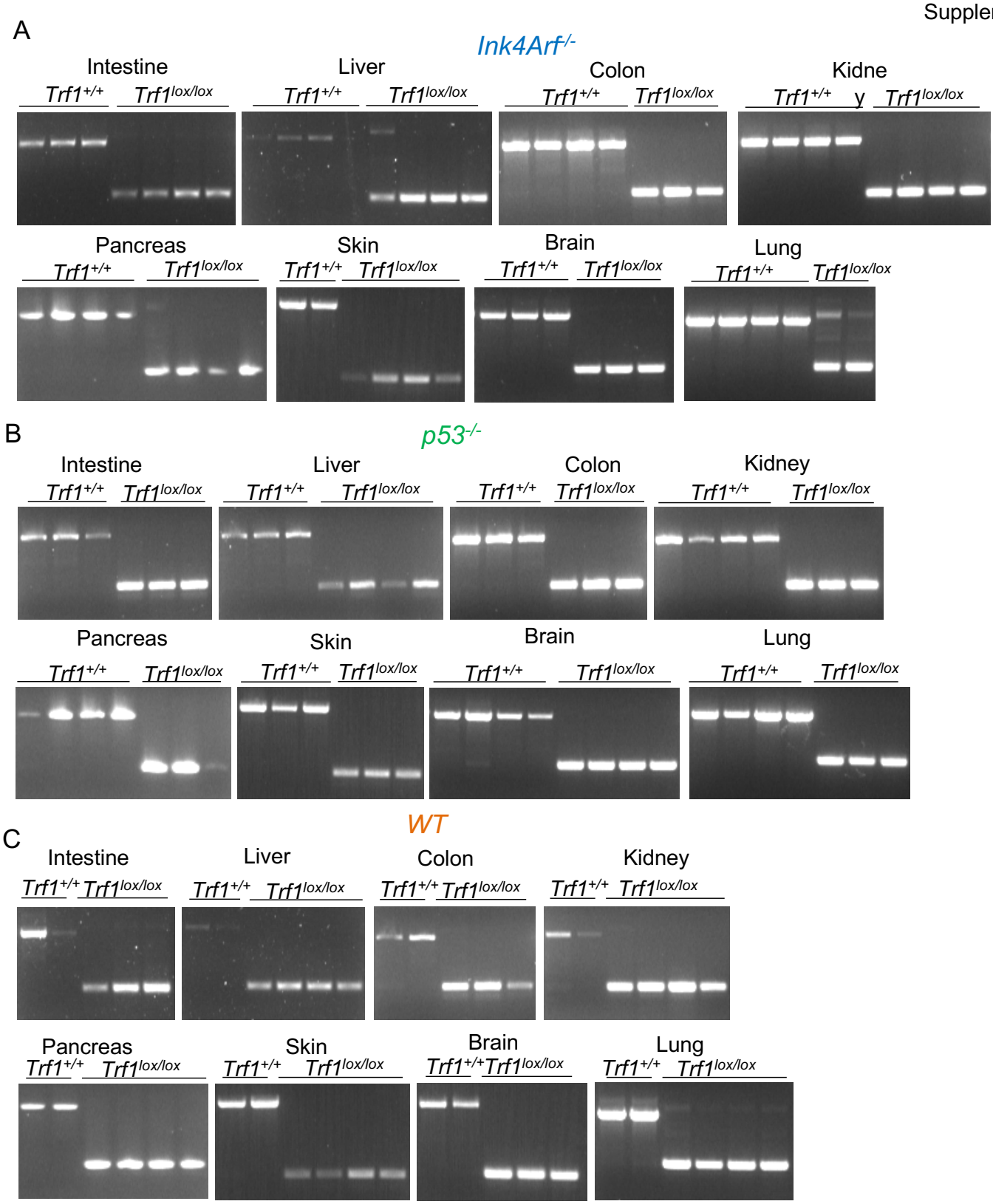
A
Ink4Arf-/-
Intestine
Trf1+/+ Trf1lox/lox
Liver
Trf1+/+ Trf1lox/lox
Colon
Trf1+/+ Trf1lox/lox
Kidne
Trf1+/+ y Trf1lox/lox
Pancreas
Trf1+/+ Trf1lox/lox
Skin
Trf1+/+ Trf1lox/lox
Brain
Trf1+/+ Trf1lox/lox
Lung
Trf1+/+ Trf1lox/lox
B
p53-/-
Intestine
Trf1+/+ Trf1lox/lox
Liver
Trf1+/+ Trf1lox/lox
Colon
Trf1+/+ Trf1lox/lox
Kidney
Trf1+/+ Trf1lox/lox
Pancreas
Trf1+/+ Trf1lox/lox
Skin
Trf1+/+ Trf1lox/lox
Brain
Trf1+/+ Trf1lox/lox
Lung
Trf1+/+ Trf1lox/lox
C
WT
Intestine
Trf1+/+ Trf1lox/lox
Liver
Trf1+/+ Trf1lox/lox
Colon
Trf1+/+ Trf1lox/lox
Kidney
Trf1+/+ Trf1lox/lox
Pancreas
Trf1+/+ Trf1lox/lox
Skin
Trf1+/+ Trf1lox/lox
Brain
Trf1+/+Trf1lox/lox
Lung
Trf1+/+ Trf1lox/lox

A

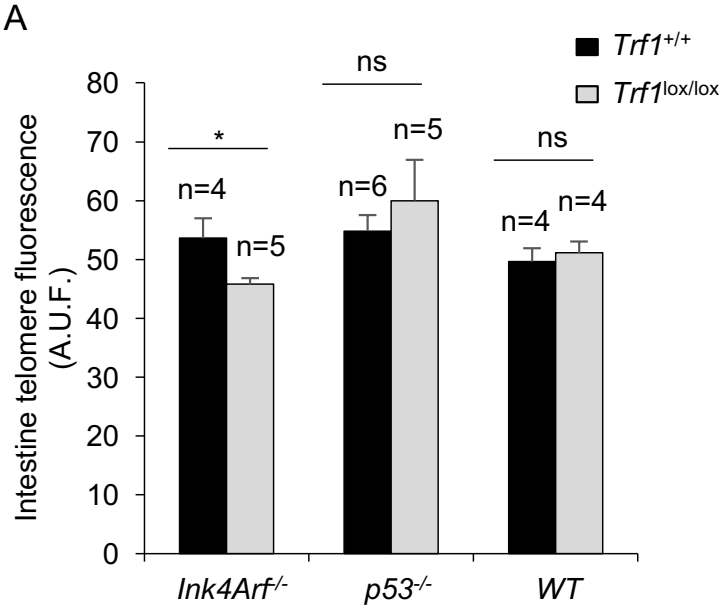
Trf1+/+
Trf1lox/lox
Intestine telomere fluorescence (A.U.F.)
80
70
60
50
40
30
20
10
0
*
ns
ns
n=4
n=5
n=6
n=5
n=4
n=4
Ink4Arf-/-
p53-/-
WT

A

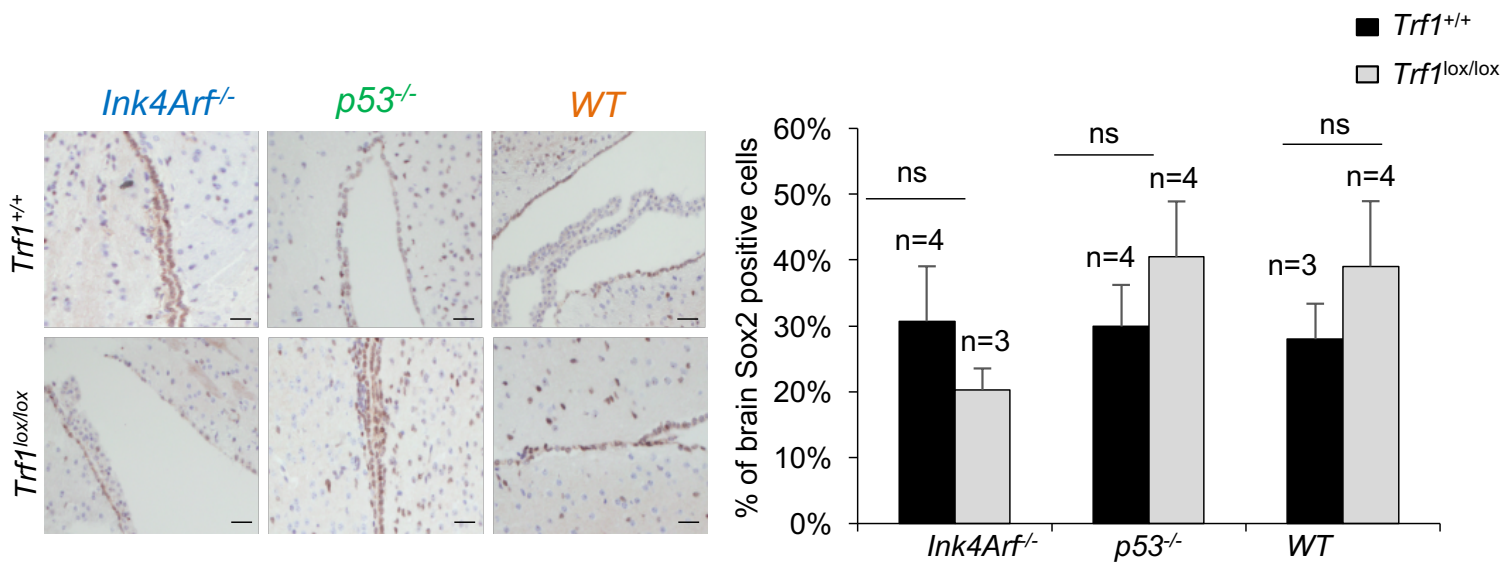
Ink4Arf-/-
p53-/-
WT
Trf1+/+
Trf1lox/lox
Trf1+/+
Trf1lox/lox
% of brain Sox2 positive cells
60%
50%
40%
30%
20%
10%
0%
ns
ns
ns
n=4
n=3
n=4
n=4
n=3
n=4
Ink4Arf-/-
p53-/-
WT

Supplemetary Figure 4

A

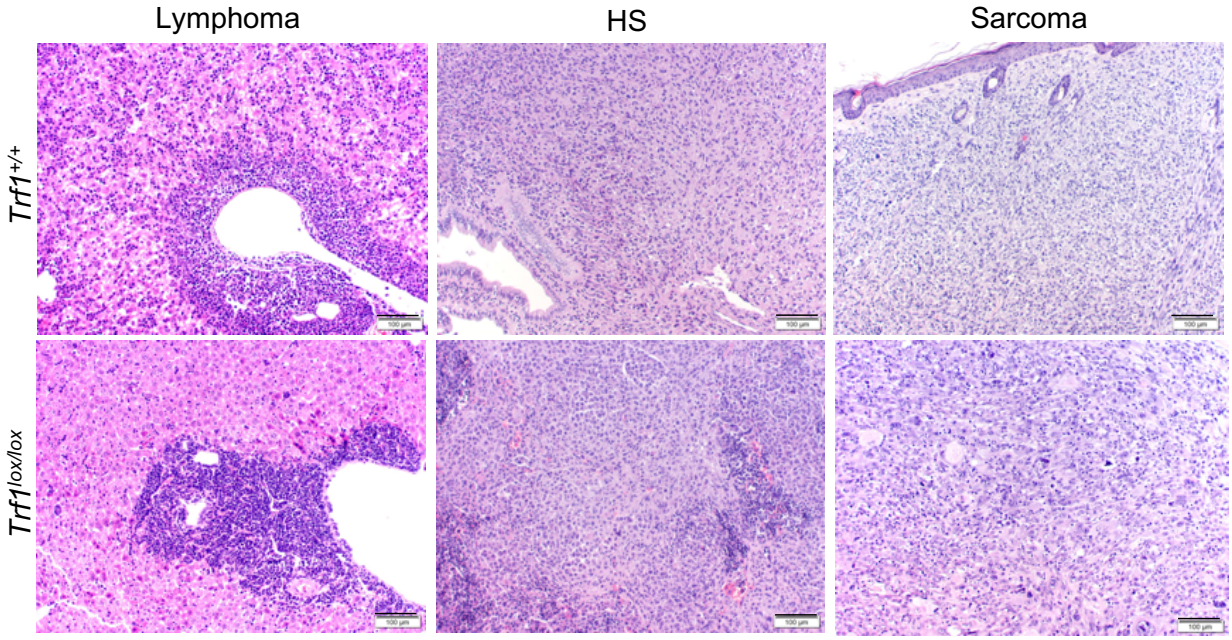

B

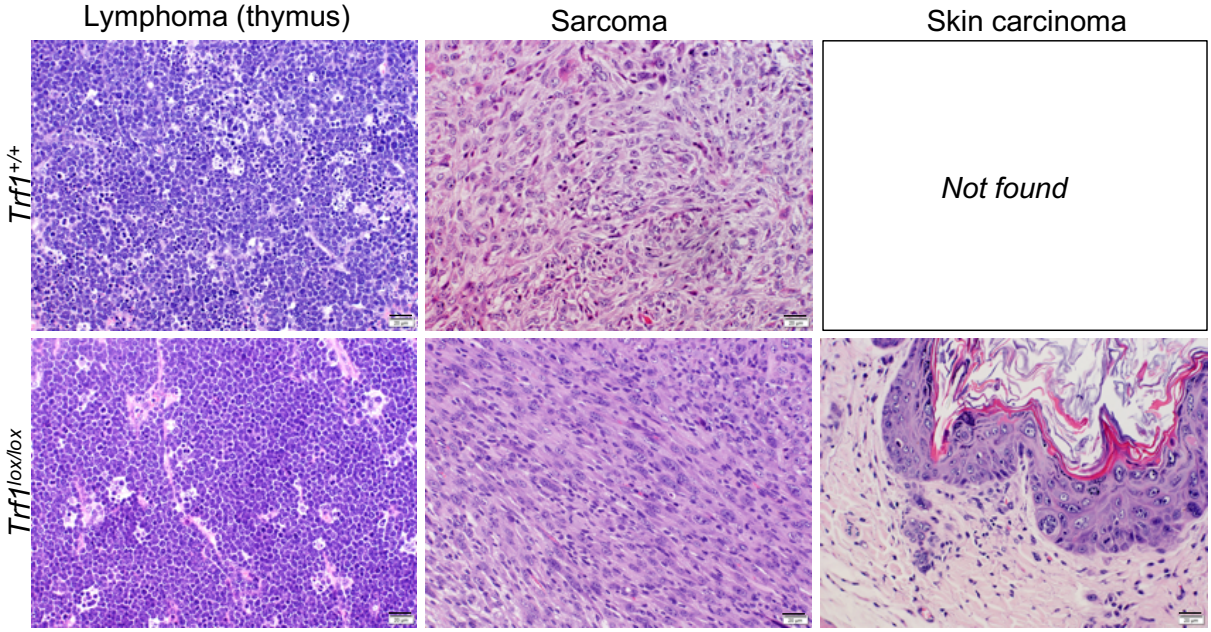

Supplementary figure legends

Supplementary Figure 1. PCR analysis of *Trf1* deletion upon tamoxifen treatment. Related to Figure 1. (A) Analysis of *Trf1* excision by PCR in *Ink4Arf*-deficient mice. (**B**) Analysis of *Trf1* excision by PCR in *p53*-deficient mice. (**C**) Analysis of *Trf1* excision by PCR in wild-type backgorund.

Supplementary Figure 2. Telomere length analysis upon *Trf1* deletion in the different genetic backgrounds. Related to Figure 1. (A) Telomere Q-FISH analysis in the intestine of the indicated genotypes. Data are represented as mean ± SEM. n represents number of mice. Statistical analysis: unpaired *t-test.*

Suplementary Figure 3. *Trf1* deletion does not decrease brain stem cell markers. Related to Figure 6. (A) Representative images (up) and quantification (down) of Sox2 -positive cells in the brain after *Trf1* deletion in the indicated backgrounds. Scale bar 20 μM. Data are represented as mean ± SEM. n represents number of mice. Statistical analysis: unpaired *t-test.*

Supplementary Figure 4. Tumor histology in *InkArf*-deficient and *p53*-deficient mice. Related to Figure 7. (A) Representative images of the different tumor types by H&E at the human end-point. Scale bar 100 μM. **(B)** Representative images of the different tumor types by H&E at the human end-point. Scale bar 20 μM.

Transparent Methods

Mice

Trf1$^{lox/lox}$ mice (Martínez *et al.*, 2009) were crossed with a mouse strain carrying ubiquitously expressed, tamoxifen-activated recombinase, *hUBC-CreERT2* (Ruzankina *et al.*, 2007) to generate *Trf1*$^{lox/lox}$ *or Trf1*$^{+/+}$*, hUBC-CreERT2* mice. These mice were further crossed with *Ink4Arf*$^{-/-}$ (Serrano *et al.*, 1996) and *p53*$^{-/-}$ (Jacks *et al.*, 1994) mouse lines to generate *Trf1*$^{+/+}$ or *Trf1*$^{lox/lox}$*, hUBC-CreERT2, Ink4Arf*$^{-/-}$ and *Trf1*$^{+/+}$ or *Trf1*$^{lox/lox}$*, hUBC-CreERT2, p53*$^{-/-}$ mice. These mice were fed *ad libitum* with tamoxifen containing diet for long-term, starting at 6 weeks of age for *p53*-deficient background and 10-weeks of age for *Ink4Arf*-deficient and wild type backgrounds. *p53*-deficient mice started tamoxifen treatment earlier due to the shorter lifespan of this mice. All mice were maintained at the Spanish National Cancer Centre under specific pathogen-free conditions in accordance with the recommendations of the Federation of European Laboratory Animal Science Associations (FELASA). All animal experiments were approved by the Ethical Committee (CEIyBA) from the Spanish National Cancer Centre and performed in accordance with the guidelines stated in the International Guiding Principles for Biomedical Research Involving Animals, developed by the Council for International Organizations of Medical Sciences (CIOMS).

Immunofluorescence analyses in tissue sections

For immunofluorescence analyses, tissues were fixed in 10% buffered formalin (Sigma) and embedded in paraffin. After despparafination and citrate antigen retrieval,

sections were permeabilized with 0.5% Triton in PBS and blocked with 1%BSA and 10% Australian FBS (GENYCELL) in PBS.

Rat polyclonal anti-TRF1 antibody (homemade) was applied overnight in antibody diluents with background reducing agents (Invitrogen). Anti-rat Alexa 555 secondary antibody (Life Technologies, S.A) was incubated 1 hr at room temperature also in antibody diluents with background reducing agents (Invitrogen).

Immunofluorescence images were obtained using a confocal ultraspectral microscope (Leica TCS-SP5). Quantifications were performed with Definiens software.

Immunohistochemistry analyses in tissue sections

For immunohistochemistry analyses, tissues were fixed in 10% buffered formalin (Sigma) and embedded in paraffin. Immunohistochemistry was performed on de-paraffinated tissue sections processed with 10 mM sodium citrate (pH 6.5) cooked under pressure for 2 min. Slides were washed in water, then in Buffer TBS Tween20 0.5 %, blocked with peroxidase, washed with TBS Tween20 0.5 % again and blocked with fetal bovine serum followed by another wash.

Primary antibodies included those raised against: γH2AX Ser 139 (Millipore), Ki67 (Master diagnostica), Sox2 (C70B1, Cell signaling) and Nestin (RAT-401, Millipore). Slides were then incubated with secondary antibodies conjugated with peroxidase from DAKO.

Pictures were taken using Olympus AX70 microscope. The percentage of positive cells was identified by eye.

Histological analyses in tissue sections

Tissue samples were fixed overnight in 10% neutral buffered formalin, embedded in paraffin and sectioned 3 µm thick and dried. Slides were dewaxed and re-hydrated through a series of graded ethanol until water and were stained with hematoxilin-eosin (H-E). Histological observations and photomicrography were performed using an Olympus DP73 digital camera. Histopathologies were classified into “non-tumoral” lesions, “preneoplasic” lesions and tumor lesions.

“Non-tumoral” lesions included degenerative lesions (atrophy in both epidermis and hypodermis, dermal fibrosis, follicular atrophy), inflammatory lesions (dermatitis, hepatitis) and proliferative lesion (benign hyperplasias, hyperkeratosis).

“Pre-neoplasic” lesions were mainly proliferative and included epithelial dysplasia, malignant hyperplasia, nuclear atypia and cell depolarization.

Tumor lesions were characterized by cellular polymorphism, irregular stratification, both loss of polarity or basement membrane disruption of epithelial cells, nuclear hyperchromatism, nuclear atypia, enlarged nucleoli, increase number of mitotic figures and atypical mitotic figures. The most frequent tumors were lymphomas (in thymus or extending and infiltrating different organs, mainly the spleen, liver, and lymph nodes), histiocytic sarcomas (in liver, spleen and mesenteric lymph nodes), subcutaneous fibrosarcomas and angiosarcomas, vertebral osteosarcomas and squamous cell carcinomas (SCC) in skin.

Telomere length analyses on tissue sections

For quantitative telomere fluorescence *in situ* hybridization (Q-FISH) we deparaffinized paraffin-embedded sections and fixed them with 4% formaldehyde, followed by digestion with pepsine/HCl and a second fixation with 4% formaldehyde. Next, we dehydrated the sides with increasing concentrations of EtOH (70%, 90%,

100% and incubated them with the telomeric probe for 3.5 min at 85ºC followed by 2h RT incubation in a wet chamber. After, the slides were extensively washed with 50% formamide and 0.08% TBS-Tween. Immunofluorescence images were obtained using a confocal ultraspectral microscope (Leica TCS-SP5) and the analysis was performed by Definiens software.

Real-time qPCR

Total RNA from frozen tissue was extracted with the RNeasy kit (QIAGEN) following manufacturer´s instructions. The cDNA synthesis was performed using the iSCRIPT cDNA synthesis kit (BIO-RAD) according to manufacturer's protocols.

Quantitative real-time PCR was performed with the QuantStudio 6 Flex (Applied Biosystems, Life Technologies) using Go-Taq qPCR master mix (Promega). All values were obtained in triplicates.

Primers for mouse samples are listed below:

TRF1-F 5'-GTCTCTGTGCCGAGCCTTC-3'

TRF1-R 5'-TCAATTGGTAAGCTGTAAGTCTGTG-3'

TBP1-F 5'-ACCCTTCACCAATGACTCCTATG-3'

TBP1-R 5'-TGACTGCAGCAAATCGCTTGG-3'

PCR

DNA from frozen tissue samples was extracted using Phenol:Chloroform:Isoamyl:Alcohol (Sigma). Cre-mediated recombination by PCR was determined using the following primers:

F: 5′-ATAGTGATCAAAATGTGGTCCTGGG-3′

R: 5′-GCTTGCCAAATTGGGTTGG-3′

125

126 **Quantification and statistical analysis**

127 Survival data were analyzed by Kaplan Meier survival curves, and comparisons
128 were performed by *Log Rank* test. Statistical analysis was performed using GraphPad
129 Prism 5.03. Comparison of the percentage of mice in Figures 3, 4, 5, 7 and 8 was
130 performed by *Chi-Square* test.

131 Immunofluorescence quantifications were performed with Definiens software
132 and immunohistochemistry quantifications were performed by direct cell counting.
133 *Unpaired Student's t test* was used to determine statistical significance. P values of
134 less than 0.05 were considered significant. Statistical analysis was performed using
135 Microsoft® Excel 2011.

136
137

References

Jacks, T., Remington, L., Williams, B. O., Schmitt, E. M., Halachmi, S., Bronson, R. T. and Weinberg, R. A. (1994) 'Tumor spectrum analysis in p53-mutant mice', *Current Biology*, 4(1), pp. 1–7. doi: 10.1016/S0960-9822(00)00002-6.

Martínez, P., Thanasoula, M., Muñoz, P., Liao, C., Tejera, A., McNees, C., Flores, J. M., Fernández-Capetillo, O., Tarsounas, M. and Blasco, M. A. (2009) 'Increased telomere fragility and fusions resulting from TRF1 deficiency lead to degenerative pathologies and increased cancer in mice', *Genes and Development*, 23(17), pp. 2060–2075. doi: 10.1101/gad.543509.

Ruzankina, Y., Pinzon-Guzman, C., Asare, A., Ong, T., Pontano, L., Cotsarelis, G., Zediak, V. P., Velez, M., Bhandoola, A. and Brown, E. J. (2007) 'Deletion of the Developmentally Essential Gene ATR in Adult Mice Leads to Age-Related Phenotypes and Stem Cell Loss', *Cell Stem Cell*, 1(1), pp. 113–126. doi: 10.1016/j.stem.2007.03.002.

Serrano, M., Lee, H. W., Chin, L., Cordon-Cardo, C., Beach, D. and DePinho, R. A. (1996) 'Role of the INK4a locus in tumor suppression and cell mortality', *Cell*, 85(1), pp. 27–37. doi: 10.1016/S0092-8674(00)81079-X.